Mechanism and Machine Theory 44 (2009) 1950–1963

Contents lists available at ScienceDirect

Mechanism and Machine Theory

journal homepage: www.elsevier.com/locate/mechmt

Myard linkage and its mobile assemblies

S.Y. Liu, Y. Chen *

School of Mechanical and Aerospace Engineering, Nanyang Technological University, 50 Nanyang Avenue, Singapore 639798, Singapore

ARTICLE INFO

Article history:
Received 28 January 2009
Received in revised form 8 May 2009
Accepted 13 May 2009
Available online 4 June 2009

Keywords:
Myard linkage
Overconstrained mechanisms
Mobile assembly
Deployable structures

ABSTRACT

In this paper, we present a way to build deployable assemblies using the Myard linkage, a three-dimensional five-bar overconstrained linkage. A family of mobile assemblies of Myard linkages with mobility one have been developed. The characteristics of the assemblies have been analysed. The result shows that they can be used as large scale deployable structures which deploy to a planar configuration and fold to a compact bundle.

1. Introduction

For close-loop linkage consisting of only links and revolute joints, generally seven links are needed to form a mobile loop according to the Kutzbach criterion [1]. All of the spatial 4*R*, 5*R* and 6*R* close-loop linkages are regarded as overconstrained simply because their mobility is due to special geometrical arrangements. These linkages have always drawn much research interest from kinematicians.

The first overconstrained mechanism which appeared in the literature was Sarrus linkage [2] in 1853. Since then, other overconstrained mechanisms have been discovered. Among them, the Bennett linkage [3,4] is the most interesting one, with only four links connected by four revolute joints whose axes are not parallel or concurrent to each other. A number of 3D overconstrained linkages are the combinations of two or more Bennett linkages, e.g., two five-bar and two six-bar Myard linkages [5], the Goldberg 5*R* and 6*R* linkages [6], the Bennett-joint 6*R* linkage [7], the Dietmaier 6*R* linkage [8] and the Wohlhart double-Goldberg linkages [9] and most recently some 6*R* linkages proposed by Baker [10] and Chen and You [11]. A most detailed study of the overconstrained mechanisms was done by Baker [12,13], etc.

In this paper, our attention is paid to the Myard's first five-bar linkage, an overconstrained 5*R* linkage. The original Myard linkage is plane-symmetric for which the two 'rectangular' Bennett chains, with one pair of twists being $\pi/2$, are symmetrically disposed before combining them [5]. Baker [14] gave the geometric condition and closure equations of the Myard linkage through the analysis of the Goldberg 5*R* linkage. So the Myard 5*R* linkage can be treated as special case of the Goldberg 5*R* linkage. Baker [15] pointed out that the Myard linkage can also be considered as a degeneracy of a plane-symmetric 6*R* linkage. Chen and You [16] have presented the extended Myard linkage, in which they reported the possibility of constructing an extended 5*R* Myard linkage by combining two complementary Bennett linkages. Unlike the original Myard linkage, the angle of twists in the Bennett linkages is not necessary to be $\pi/2$. In a previous study it has been found that the Myard linkages can be used as deployable units for the construction of an umbrella-shaped deployable structure [17]. Here

* Corresponding author. Tel.: +65 6790 5941; fax: +65 6790 4062.
E-mail address: chenyan@ntu.edu.sg (Y. Chen).

0094-114X/$ - see front matter © 2009 Elsevier Ltd. All rights reserved.
doi:10.1016/j.mechmachtheory.2009.05.001

we present a new method to construct a family of mobile assemblies of Myard linkage unlimitedly using tilings and patterns [18].

The layout of this paper is as follows. First, in Section 2 we introduce a Myard's first five-bar linkage constructed by combining two Bennett linkages and its closure equations. Then in Section 3 we describe in detail the construction of mobile assemblies and analyse their geometric characteristics. Section 4 presents a method for the model fabrication. And further discussions in Section 5 conclude the paper.

2. Myard linkage

Fig. 1 shows a Myard's first five-bar linkage constructed by combining the two 'rectangular' Bennett chains, with one pair of twists being $\pi/2$. The Bennett linkages 1236 and 5164 are first disposed as mirror images of each other before combining them. Then the common links 16 and 63 (or 64) and joint 6 are removed to form a 5*R* plane-symmetric overconstrained linkage with the mirror coincident with the plane of symmetry. So the conditions on its geometric parameters are

$$a_{34} = 0, \quad a_{12} = a_{51}, \quad a_{23} = a_{45}, \tag{1a}$$

$$\alpha_{23} = \alpha_{45} = \frac{\pi}{2}, \quad \alpha_{51} = \pi - \alpha_{12}, \quad \alpha_{34} = \pi - 2\alpha_{12}, \tag{1b}$$

$$R_i = 0 \quad (i = 1, 2, \ldots, 5) \tag{1c}$$

and

$$a_{12} = a_{23} \sin \alpha_{12} \tag{1d}$$

due to the geometric condition of the Bennett linkage [3,4]. Here, $a_{i(i+1)}$ is the distance between adjacent joint axes, which is also referred as length of link $i(i+1)$. $\alpha_{i(i+1)}$ is the rotation angle between adjacent joint axes positively about the axis of joint i, which is also referred as twist of link $i(i+1)$. R_i is the distance from link $(i-1)i$ to link $i(i+1)$ positively about the joint axis, which is also referred as offset of joint i. And θ_i is the revolute variable of the linkage, which is the angle of rotation from link $(i-1)i$ to link $i(i+1)$ positively about the axis of joint i .

The closure equations are [14,16]:

$$\varphi_1 + \varphi_3 + \varphi_4 = 2\pi, \tag{2a}$$

$$\varphi_2 + \varphi_5 = 2\pi, \tag{2b}$$

$$\tan\frac{\varphi_4}{2} \tan\frac{\varphi_5}{2} = \frac{\sin\frac{1}{2}\left(\frac{\pi}{2} + \alpha_{12}\right)}{\sin\frac{1}{2}\left(\frac{\pi}{2} - \alpha_{12}\right)} \tag{2c}$$

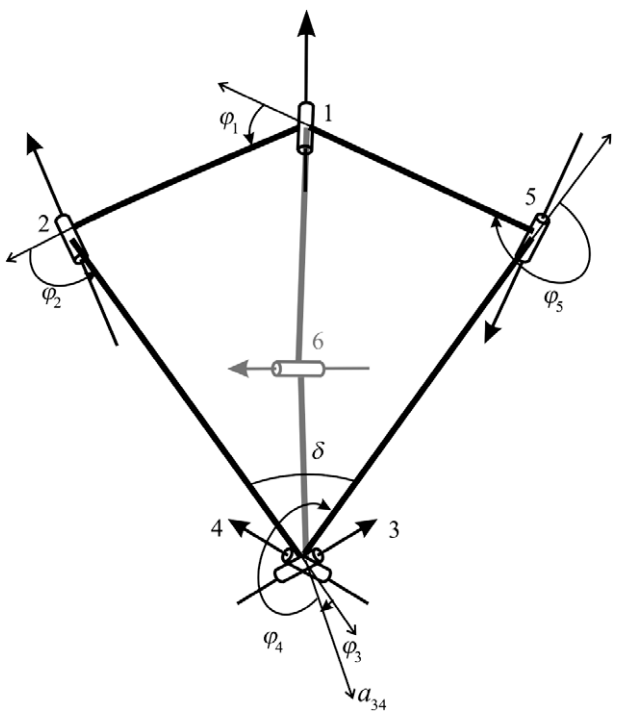

Fig. 1. Construction of Myard Linkage.

and

$$\tan\frac{\varphi_2}{2}=\frac{\sin\frac{1}{2}\left(\frac{\pi}{2}+\alpha_{12}\right)}{\sin\frac{1}{2}\left(\frac{\pi}{2}-\alpha_{12}\right)}\tan\frac{\varphi_3}{2}. \tag{2d}$$

From (2c) and (2d), it is obtained that

$$\varphi_4=\varphi_3+\pi.$$

A set of kinematic paths of a Myard linkage is shown in Fig. 2, in which $\alpha_{12}=\pi/3$.

It can be noted from Fig. 2 that φ_1 changes 4π in one full cycle of the linkage. However, the physical model in Fig. 3 reveals that φ_1 can only change between $-\pi$ and π, while $\varphi_1\in(-2\pi,-\pi)$ and $\varphi_1\in(\pi,2\pi)$ is corresponding to the symmetric configuration of $\varphi_1\in(-\pi,\pi)$ about the symmetry plane, i.e. links 23 and 45 exchange positions, so do links 12 and 51. Set the angle between links 23 and 45 as δ, then the relationship between φ_1 and δ can be derived from $\Delta125$ and $\Delta23(4)5$ in Fig. 1 as

$$a_{12}^2+a_{12}^2-2a_{12}^2\cos(\varphi_1-\pi)=a_{23}^2+a_{23}^2-2a_{23}^2\cos\delta.$$

Considering (1d), we have

$$\sin^2\alpha_{12}(1+\cos\varphi_1)=1-\cos\delta, \tag{3}$$

which is plotted in Fig. 4 for $-\pi\leqslant\varphi_1\leqslant\pi$.

From Figs. 2 and 4, three important configurations exist regardless of the value of α_{12}:

(i) $\varphi_1=\pi$, $\varphi_2=\varphi_3=0$, $\varphi_4=\pi$, $\varphi_5=0$ (or 2π), and $\delta=0$, which is the configuration that the linkage forms a straight line with the length $a_{12}+a_{23}$, see Fig. 3a;

(ii) $\varphi_1=0$, $\varphi_2=\pi/2+\alpha_{12}$, $\varphi_3=\pi/2$, $\varphi_4=3\pi/2$, $\varphi_5=3\pi/2-\alpha_{12}$, and $\delta=2\alpha_{12}$, which is the configuration that the linkage form a planar triangle with inner angle being $2\alpha_{12}$, $\pi/2-\alpha_{12}$, $\pi/2-\alpha_{12}$, and side lengths being $2a_{12}$, a_{23}, a_{23}, see Fig. 3c;

(iii) $\varphi_1=-\pi$, $\varphi_2=\varphi_3=\varphi_5=\pi$, $\varphi_4=0$ (or 2π), and $\delta=0$, which is the configuration that the linkage forms a straight line with the length $a_{23}=a_{12}/\sin\alpha_{12}$ as shown in Fig. 3e.

If using the Myard linkage as a basic unit to construct a deployable structure, configurations (i) and (iii) correspond to the folded configurations while configuration (ii) is the deployed one. Therefore, this linkage is an ideal unit for large deployable structures.

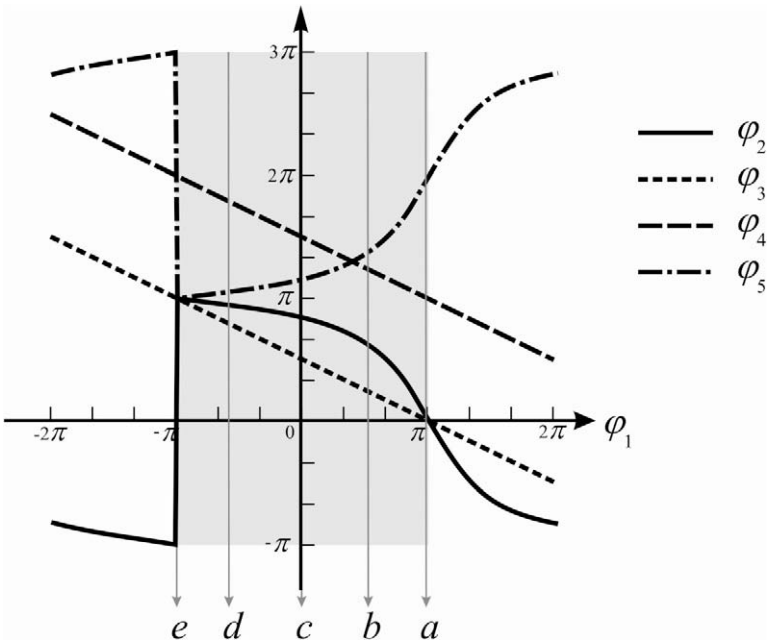

Fig. 2. The kinematic paths of Myard linkage for $\alpha_{12}=\pi/3$ ('*a*'–'*e*' are to indicate the five configurations of the model in Fig. 3).

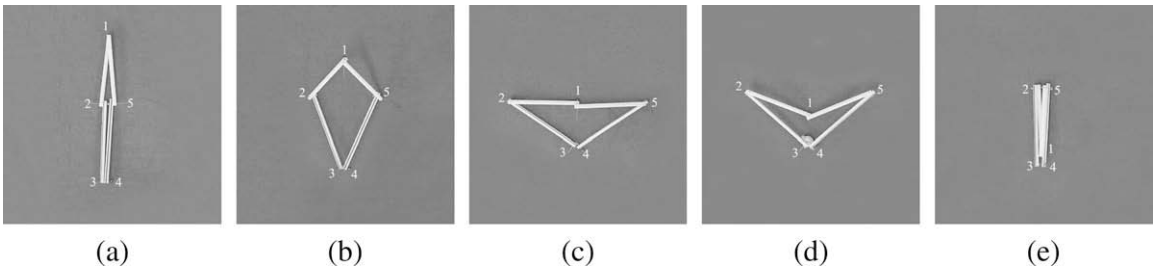

Fig. 3. Motion sequence of a Myard linkage with $\alpha_{12} = \pi/3$.

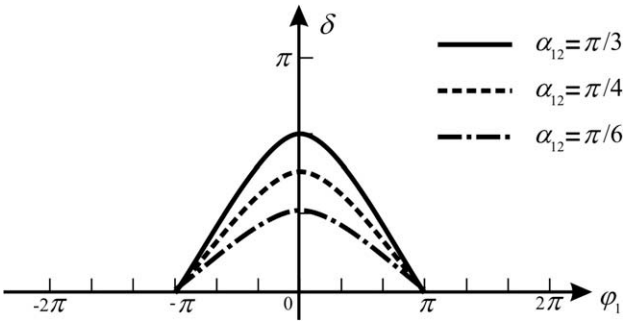

Fig. 4. The relationship between φ_1 and δ.

3. Mobile assemblies of Myard linkage

Briand and You [17] have used Myard linkages as deployable units to build an umbrella-shaped deployable structure as shown in Fig. 5. When the assembly consists of n identical Myard linkages, there are n joints at the centre point O. Because the frame forms a flat polygon when fully deployed with each Myard linkage forms a triangle, the twist of each Myard linkage must satisfy that $\alpha_{12} = \pi/n$.

Meanwhile, we find that two Myard linkages can be assembled together by a pair of continuous cross-bars as links 12 and 51 for both linkages, as shown in Fig. 6. The cross-bars intersect at point P, which is the position of joint 1 for both linkages. Two Myard linkages, MLa and MLb, will move in a synchronised manner, i.e. both reach the folded and deployed configurations at same time, even when two α_{12}'s are not equal, due to the relationship between φ_1 and δ shown in Fig. 4. MLa and MLb share the same symmetry plane, which is the vertical plane passing through joint 1 and links 34 of both linkages. A model is shown in Fig. 7.

It is interesting to note that when the twists of MLa and MLb are the same, the assembly is symmetric about point P. The axis of joint 1 of MLa and that of MLb are in the opposite directions. The assembly has a symmetry plane and a symmetry point, which is on the symmetry plane. Thus the assembly also has a two-fold rotational symmetry, C_2, which is about the axis perpendicular to the symmetry plane at point P, see Fig. 6. As a result, the planes formed by joint axes 3 and 4 of MLa and MLb are always parallel during the movement of the assembly. This particular characteristic makes it possible to construct an unlimited number of Myard linkages into a family of mobile assemblies by combining above two kinds of assemblies to-

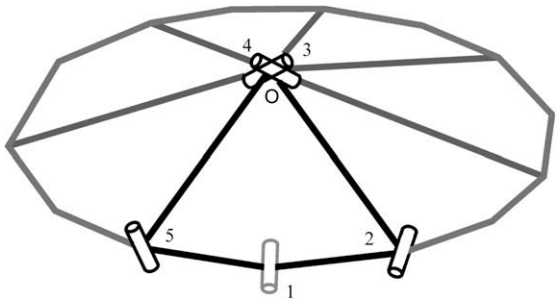

Fig. 5. A schematic diagram for an umbrella-like deployable frame made from seven Myard linkages. Only one of the Myard linkages is highlighted.

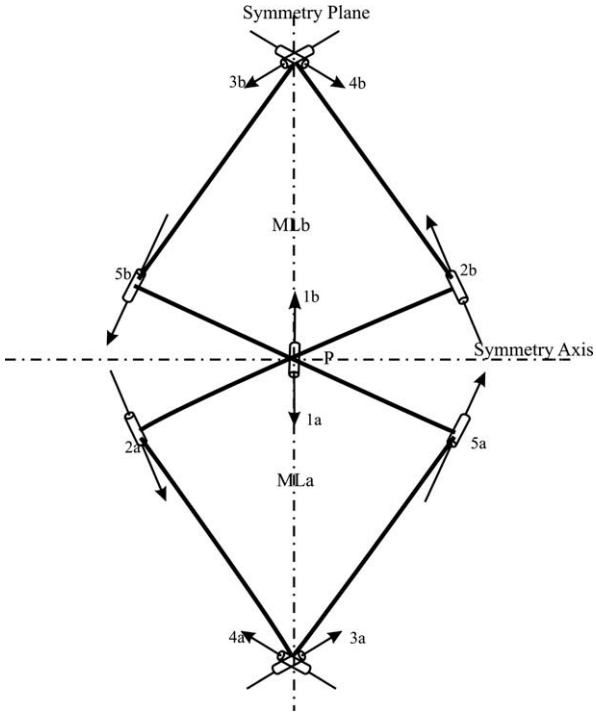

Fig. 6. A schematic diagram of a mobile assembly of two Myard linkages.

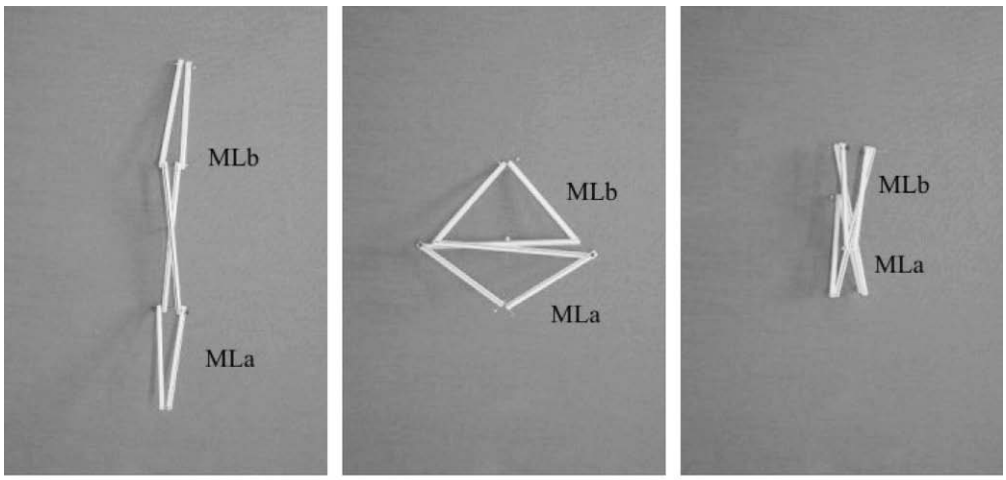

Fig. 7. The mobile sequence of the assembly of two Myard linkages with $\alpha_{12} = \pi/3$ for MLa and $\alpha_{12} = 3\pi/4$ for MLb.

gether using tilings and patterns [18]. A number of umbrella-shaped assemblies can be connected together through the cross-bars to form a large assembly while the internal mobility is kept. Because the umbrella-shaped assembly deploys into regular polygons, the tilings with the regular polygons should be considered as connection patterns.

Mathematically, the tilings accommodating regular polygons can be classified into four types: regular and uniform tilings, *k*-uniform tilings, equitransitive and edge-transitive tilings, and tilings that are not edge-to-edge. The only edge-to-edge monohedral tilings by regular polygons are three regular tilings, (3^6), (4^4), and (6^3), shown in Fig. 8, where the basic tiles are identical equilateral triangles, squares and regular hexagons, respectively. In order to maintain the character that two planes formed by joints 3 and 4 are parallel, all the Myard linkages in the assembly must be identical so that the regular polygons in assembly will also be identical. Hence, only three types of monohedral tilings can be used. When the umbrel-

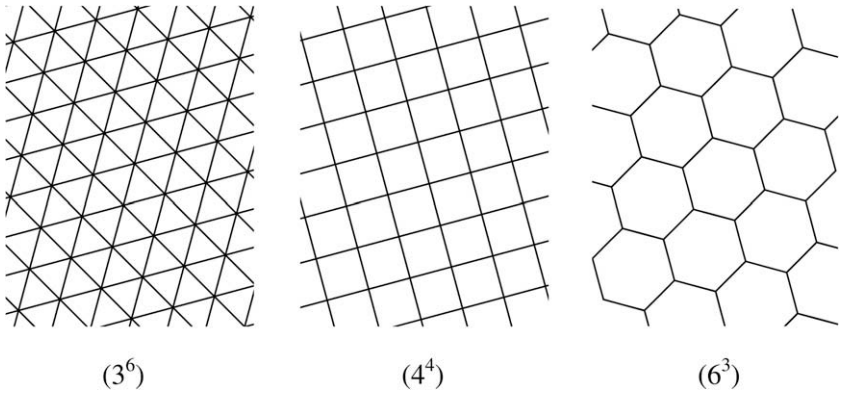

Fig. 8. The edge-to-edge monohedral tilings by regular polygons.

la-shaped assembly forms an equilateral triangle in its deployed configuration, the twist of Myard linkage should be $\alpha_{12} = \pi/3$. When the umbrella-shaped assembly has a square profile, the twist of Myard linkage should be $\alpha_{12} = \pi/4$. And when the profile of an umbrella-shaped assembly is a regular hexagon, the twist of Myard linkage should be $\alpha_{12} = \pi/6$. Next, we should show how to construct these three types of assemblies.

3.1. Assembly I

Three Myard linkages with $\alpha_{12} = \pi/3$ can form an assembly block that deploys into an equilateral triangle, see Fig. 9a. Based on tiling (3^6), a number of such blocks can be assembled through the continuous cross-bars, see Fig. 9b. The assembly is mobile because all of the Myard linkages are identical and they move synchronously, which is demonstrated by the model in Fig. 10. When the assembly is placed horizontally, the unit centres move upwards or downwards. That is, in Fig. 9b, O_1, O_3 and O_5 move upwards together, whereas O_2, O_4 and O_6 move downwards together, as shown in Fig. 10d.

3.2. Assembly II

Similarly, four Myard linkages with $\alpha_{12} = \pi/4$ can form an assembly block, and further form a mobile assembly following tiling (4^4), see Fig. 11, in which all the Myard linkage move synchronously as shown in Fig. 12, where the centres in the squares with the same colour will move upwards or downwards together.

3.3. Assembly III

Six Myard linkages with $\alpha_{12} = \pi/6$ can be put together to form an umbrella frame shown in Fig. 13a. The assembly has a mobility one. Furthermore, a larger mobile block can be made in a way similar to those used to form assemblies I and II, using it as a deployable block. Adjacent Myard linkages with $\alpha_{12} = \pi/6$ are joined together by a pair of cross-bars, see Fig. 13b. The

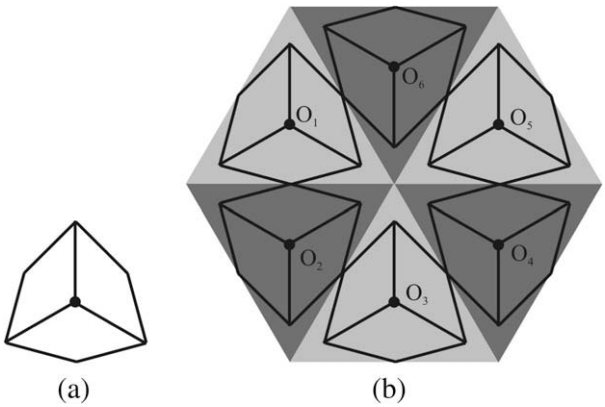

Fig. 9. The assembly of Myard linkages with $\alpha_{12} = \pi/3$. (a) An assembly of three such linkages as a unit; (b) assembly with six units.

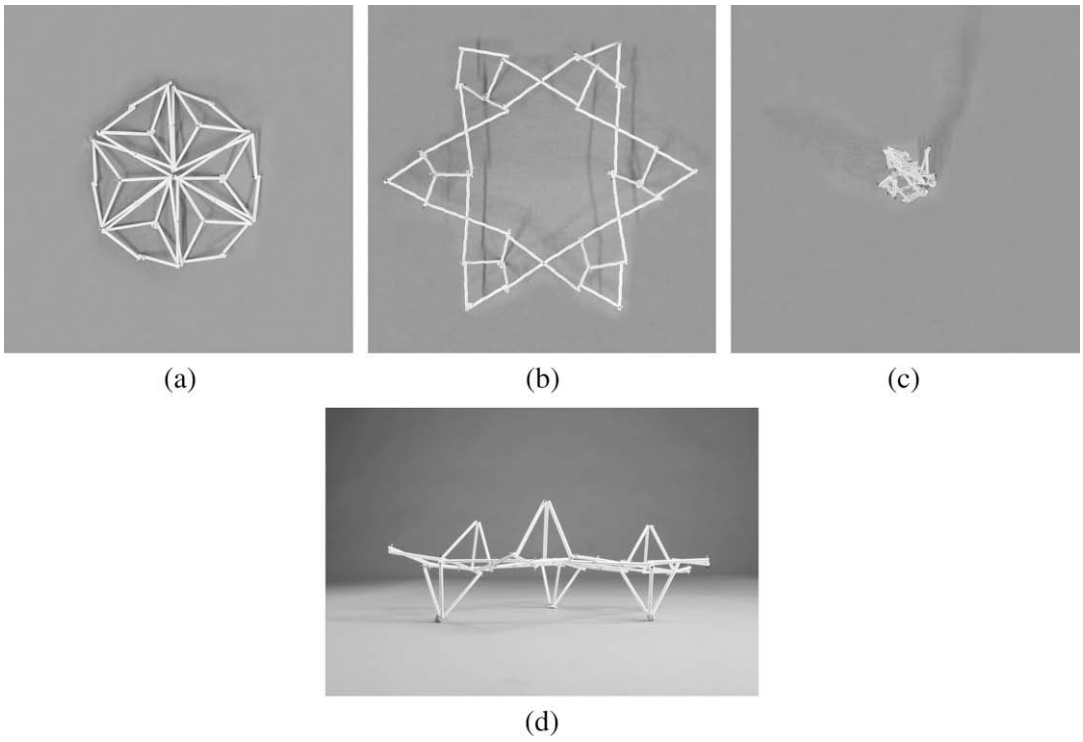

Fig. 10. The motion sequence of a model of mobile assembly with $\alpha_{12} = \pi/3$. (a)–(c) top views; (d) side view.

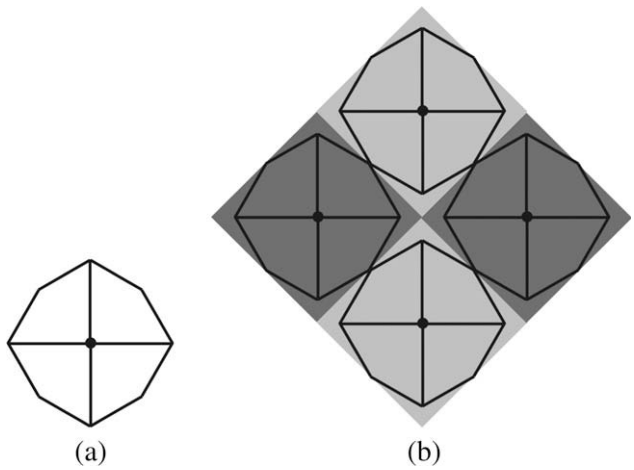

Fig. 11. The assembly of Myard linkages with $\alpha_{12} = \pi/4$. (a) An assembly of four such linkages as a unit; (b) assembly with four units.

assembly still has a mobility one. When centre C moves upwards during deployment, $C_i\,(i = 1, 2, \ldots, 6)$ move downwards. Next following tiling (6^3), three larger blocks are assembled together as shown in Fig. 13c. The resulting assembly is mobile but has more than mobility one because there are only three Myard linkages around point A, which can move independently. In order to synchronise their motions, three pairs of bars, shown in dash line in Fig. 13c, are added so that there are a total of six Myard linkages around point A to form an umbrella frame. Now the whole assembly has only a mobility one. This construction process can be used repeatedly to form a large deployable structure. If the centre joints in the centre of hexagons move together upwards, the centre joints in the corners of hexagons will move together downwards. A model is shown in Fig. 14. It should be noticed that the bars in dash links do not form cross-bars. If they are replaced by cross-bars, the assembly loses its mobility. As shown in Fig. 13c, if the umbrella-shaped assemblies centred by A and B are connected by a pair of

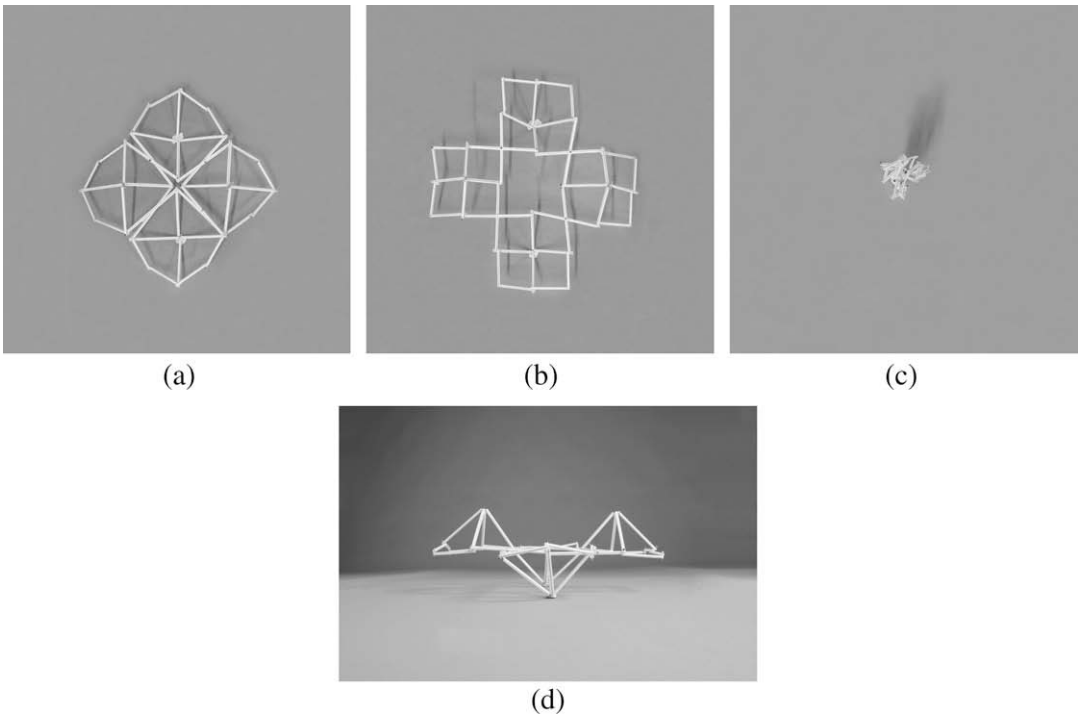

Fig. 12. The motion sequence of a model of mobile assembly with $\alpha_{12} = \pi/4$. (a)–(c) top views; (d) side view.

cross-bars, centre joint A moves downwards while B moves upwards, which conflicts with the fact that the centre joints in the corners of hexagons will move together downwards. Hence, the whole assembly cannot move.

As discussed in the previous section, a single Myard linkage deploys to a planar triangle and folds to a bundle. This character remains in the mobile assemblies I, II, and III, the final assemblies can deploy into a planar profile and fold to a bundle. During the motion, all the centre joints form two planes parallel to the deployed plane. The distance between the upper and lower joints, H_a, and the dimension of frame's projection, D_a, change with kinematic variable, φ_1. These two sets of relationship can be found by analysing the assembly of two Myard linkages connected by a pair of cross-bars as shown in Fig. 15. MLa and MLb have the same link length and twist. So joints 3 and 4 of MLa meet at point M and form a horizontal plane, and joints 3 and 4 of MLb meet at point N and form another horizontal plane. Because two Myard linkages are identical, they have the same symmetry plane which is the vertical plane passing through MN and joint 1. MN intersects joint 1 at point P, and projects P on two horizontal planes at point S and T. Then $\overline{ST} = 2\overline{PS}$ is the vertical distance between M and N, denoted by H, while $\overline{MS} + \overline{NT} = 2\overline{MS}$ is the horizontal distance between M and N, denoted by D. The relationship between H, D and the kinematic variable φ_1 can be found in terms of geometric parameters of the Myard linkage, a_{12} and α_{12} .

For MLa in Fig. 15, axis 2 is certainly perpendicular to links 12 and 23, i.e.,

$$\text{axis } 2 \perp \text{PQ} \quad \text{and} \quad \text{axis } 2 \perp \text{QM},$$

which means axis 2 is perpendicular to the plane MPQ. Because $\alpha_{23} = \frac{\pi}{2}$, axis 2 is perpendicular to axis 3, i.e.,

$$\text{axis } 2 \perp \text{MR}.$$

MR must be on the plane MPQ. As axis 3 is perpendicular to link 23, $\angle\text{QMR} = \pi/2$. Therefore,

$$\angle\text{PMR} = \pi/2 - \angle\text{QMP}. \tag{4}$$

For the triangle ΔMPQ, $\angle\text{PQM} = \pi - \varphi_2$, and $\overline{PQ} = a_{12}$, $\overline{MQ} = a_{23} = \frac{a_{12}}{\sin\alpha_{12}}$. Then

$$\overline{MP} = a_{12}\sqrt{1 + \frac{1}{\sin^2\alpha_{12}} + 2\frac{\cos\varphi_2}{\sin\alpha_{12}}}, \tag{5}$$

and

$$\sin\angle\text{QMP} = \frac{\sin\varphi_2}{\sqrt{1 + \frac{1}{\sin^2\alpha_{12}} + 2\frac{\cos\varphi_2}{\sin\alpha_{12}}}}. \tag{6}$$

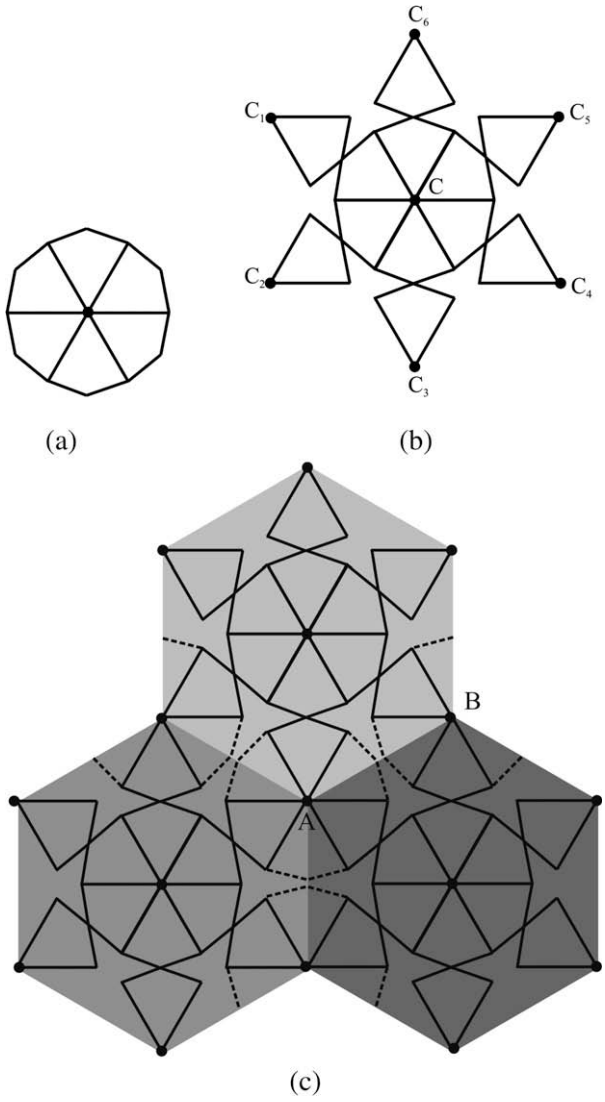

Fig. 13. Assembly of Myard linkage with $\alpha_{12} = \pi/6$. (a) An assembly of six such linkages; (b) a unit; (c) assembly with three units.

In Fig. 15, because PS is perpendicular to horizontal plane, PS $\perp$ MR. Let RS $\perp$ MR, then PR $\perp$ MR. So For the triangle ΔPMR,

$$\overline{\mathrm{MR}} = \overline{\mathrm{MP}} \cos \angle \mathrm{PMR}. \tag{7}$$

Considering (4), (5), and (7) becomes,

$$\overline{\mathrm{MR}} = a_{12} \sin \varphi_2. \tag{8}$$

For the triangle ΔMRS, $\angle \mathrm{RMS} = \frac{1}{2}\alpha_{34} = \frac{\pi}{2} - \alpha_{12}$,

$$\overline{\mathrm{MS}} = \frac{\overline{\mathrm{MR}}}{\cos \angle \mathrm{RMS}} a_{12} \frac{\sin \varphi_2}{\sin \alpha_{12}}. \tag{9}$$

For the triangle ΔPMS,

$$\overline{\mathrm{PS}} = \sqrt{\overline{\mathrm{MP}^2} - \overline{\mathrm{MS}^2}} = a_{12}\left(1 + \frac{\cos \varphi_2}{\sin \alpha_{12}}\right). \tag{10}$$

So the vertical distance between M and N is

$$H = 2 \cdot \overline{\mathrm{PS}} = 2a_{12}\left(1 + \frac{\cos \varphi_2}{\sin \alpha_{12}}\right), \tag{11}$$

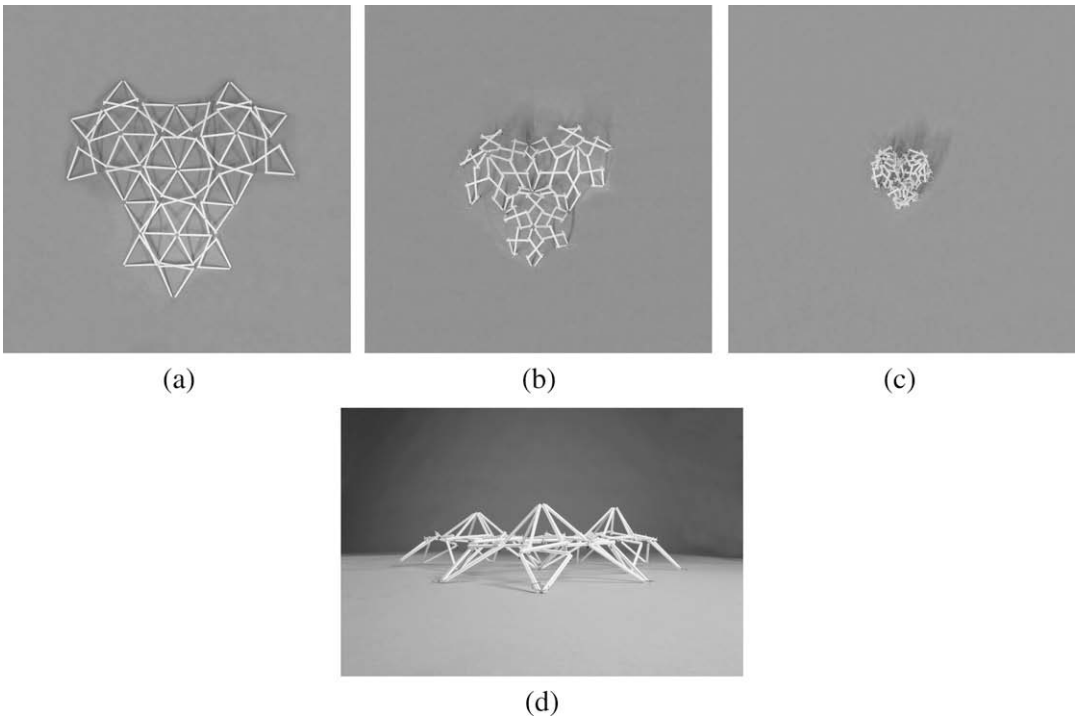

Fig. 14. The motion sequence of a model of mobile assembly with $\alpha_{12} = \pi/6$. (a)–(c) top views; (d) side view.

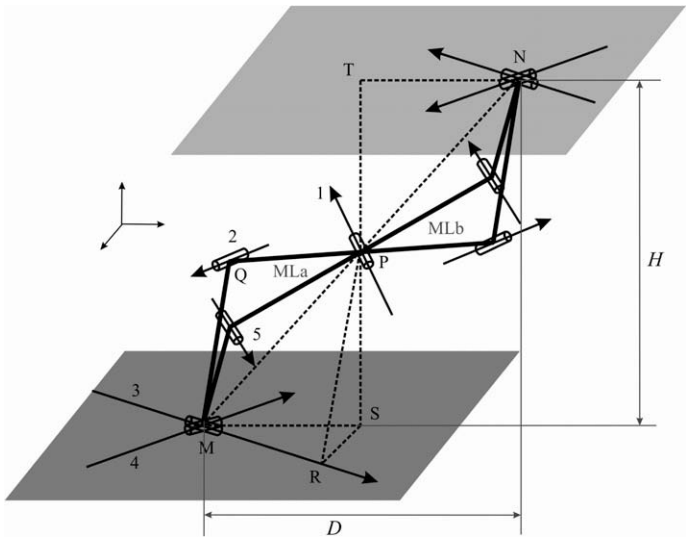

Fig. 15. A schematic diagram of a mobile assembly of two same Myard linkages.

and the horizontal distance between M and N is

$$D = 2 \cdot \overline{\mathrm{MS}} = 2a_{12}\frac{\sin\varphi_2}{\sin\alpha_{12}}. \tag{12}$$

According to (2a), (2c), and (2d),

$$\varphi_2 = 2\arctan\left[\frac{\sin\frac{1}{2}(\frac{\pi}{2}+\alpha_{12})}{\sin\frac{1}{2}(\frac{\pi}{2}-\alpha_{12})}\tan\frac{(\pi-\varphi_1)}{4}\right]. \tag{13}$$

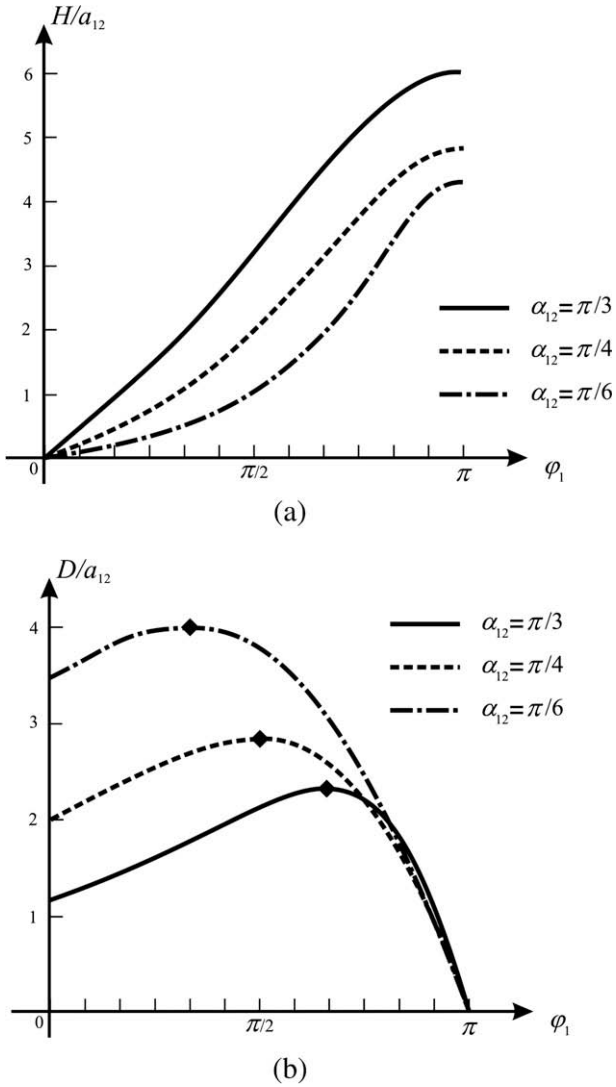

Fig. 16. H/a_{12} and D/a_{12} vs. φ_1 in the range of 0 to π for different α_{12} .

Substituting (13) into (11) and (12), the relationship between H, D and φ_1 can be obtained. For the assembly shown in Fig. 15, φ_1 changes either between 0 and π or between $-\pi$ and 0, when the physical size of the cross-bars is considered. Fig. 7c shows that when $-\pi \leqslant \varphi_1 < 0$, H is not the total height of assembly, and two parallel planes are not top and bottom planes of the assembly. And the assembly is difficult to design resulting in little application potential. As a result, we become more interested in the behaviour of the assembly for $0 \leqslant \varphi_1 < \pi$. Fig. 16 shows the plots of H/a_{12} and D/a_{12} vs. φ_1 in the range of 0 to π for different α_{12} because H and D are proportional to a_{12}. It is noticed that H/a_{12} increases from 0 to $2(1+\frac{1}{\sin\alpha_{12}})$ when $0 \leqslant \varphi_1 < \pi$, while D/a_{12} increases first from $2\cot\alpha_{12}$ to $2/\sin\alpha_{12}$ when φ_1 changes from 0 to $2\alpha_{12}$ and then decreases from $2/\sin\alpha_{12}$ to 0 when φ_1 goes from $2\alpha_{12}$ to π. For whole assembly, $H_a = H$ and D_a is proportional to D. The proportional ratio, $R_a = D_a/D$, varies with the number of units in the assembly. Thus there are three interesting configurations:

(i) $\varphi_1 = 0, H_a = 0$ and $D_a = (2a_{12}\cot\alpha_{12}) \cdot R_a$, where the whole assembly forms a plane while each unit forms a equilateral triangle, square or regular hexagon.

(ii) $\varphi_1 = 2\alpha_{12}$, $\varphi_2 = \pi/2$, $H_a = 2a_{12}$ and $D_a = (2a_{12}/\sin\alpha_{12}) \cdot R_a$, where the assembly has the largest horizontal dimension, which is marked as ♦ in Fig. 9b, and the cross-bar also forms a horizontal plane, see the side views in Figs. 10, 12 and 14.

(iii) $\varphi_1 = \pi$, $H_a = 2a_{12}(1+\frac{1}{\sin\alpha_{12}})$ and $D_a = 0$, where the assembly folds into a bundle with all links collinear.

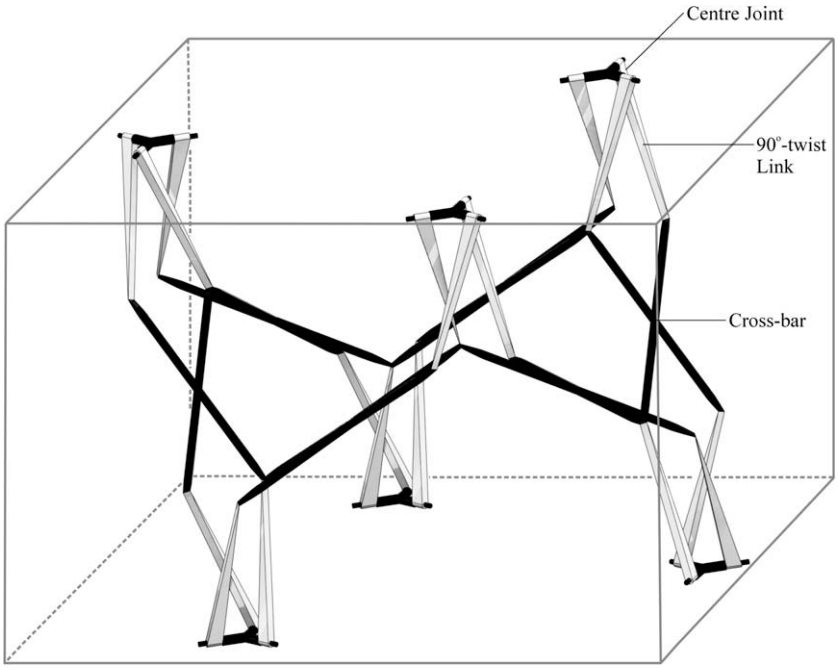

Fig. 17. A prototype of mobile assembly with $\alpha_{12} = \pi/3$.

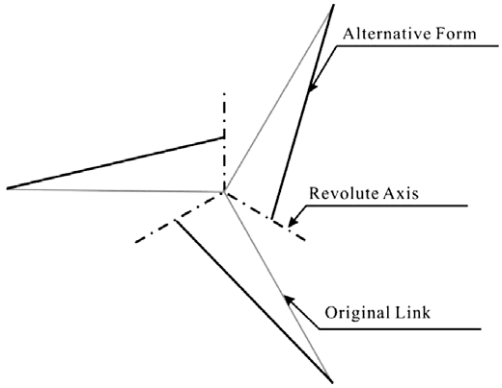

Fig. 18. A schematic drawing of the centre joint and 90-degree-twist link.

4. Model design

It should be pointed out that the physical cross-sectional sizes of the links and joints of linkage are always ignored when conducting the kinematic analysis. And links always span the shortest distance between two adjacent revolute hinges. We cannot do so when designing a prototype for certain applications. As the result, we had to extend the joint axes and connect them by links which are no long perpendicular to the joint axes. We call such linkage the alternative form of the original linkage. A prototype of assembly of Myard linkages with $\alpha_{12} = \pi/3$ is shown in Fig. 17, which was designed with Solidworks®. The design consists of three major components, namely, the centre joint, the 90°-twist link and the cross bars. The centre joint is a connector with three axes at 120° apart, and it is connected to three 90°-twist links by revolute joints. As shown Fig. 18, this combination is equivalent to the original links which intersect at the centre. The motion sequence of the prototype is shown in Fig. 19. In Fig. 19a and b, the assembly is in its deployed configuration where φ_1 is close to 0 and all the links are almost co-planar. In Fig. 19c and d, $\varphi_1 = 2\pi/3$, the assembly spans the largest area. In Fig. 19e and f, φ_1 is close to π, the assembly folds into a bundle. Similar design can be done for assemblies with $\alpha_{12} = \pi/4$ and $\alpha_{12} = \pi/6$.

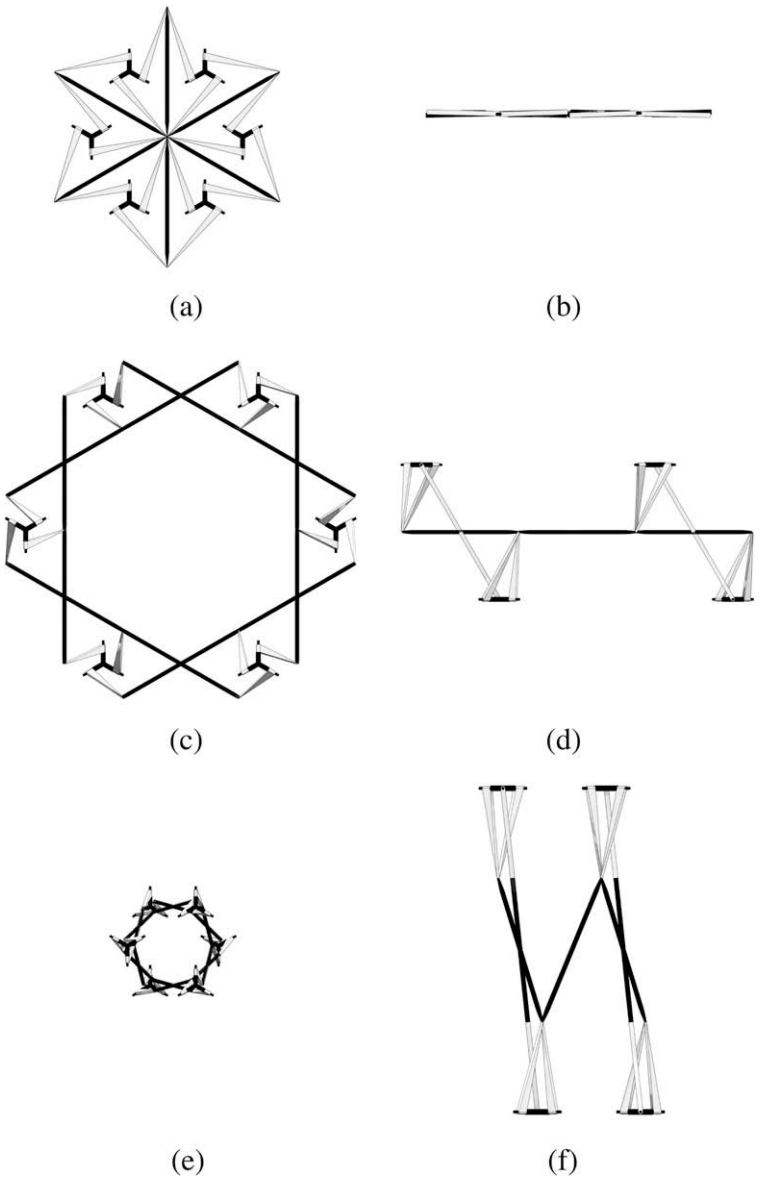

Fig. 19. The motion sequence of a prototype of mobile assembly with $\alpha_{12} = \pi/3$. (a), (c), (e) Top views; (b), (d), (f), front views.

5. Conclusion and discussion

In this paper, we have created a number of deployable blocks based on the Myard linkage. With these blocks, we can build large deployable assemblies. Because we use cross-bars to synchronise the motion of each deployable blocks, the resulting assemblies has only a mobility one. In the deployed configuration, the top or bottom joints form two parallel planes whereas the assemblies becomes a compact bundle when folded, showing their potential as large aerospace deployable frames. The characteristics of the assemblies have been analysed. It has been found that when deployed, the distance between the parallel planes and dimension of the assembly projected on the parallel planes vary with the kinematic variables. This special characteristic makes it possible to use the assembly as the supporting system for flexible skin or solid sliding shells that are attached to the centre joints.

The dimension of such assemblies varies with the kinematic variables. When φ_1 changes from 0 to $2\alpha_{12}$, both thickness and area of the assembly increase, while when φ_1 changes from $2\alpha_{12}$ to π, the thickness increases as the area of the structure decreases. So in the first range, the overall assembly exhibits negative Poisson ratio in three dimensions.

We have considered three assemblies using Myard linkages with $\alpha_{12} = \pi/3$, $\alpha_{12} = \pi/4$, and $\alpha_{12} = \pi/6$ following monohedral tilings (3^6), (4^4) and (6^3), respectively. For potential applications of these assemblies, detailed structural analysis should

be performed to select which set of twist and tiling is more suitable. Meanwhile, the actuation of the assemblies also should be analysed. Although we use φ_1 as input in the kinematic analysis, it is possible to actuate other revolute joints or even use linear actuators for deployment. It also should be pointed out that the deployed configuration discussed in Section 3 is a limiting configuration on the kinematic path of the assembly rather than the configuration with the maximum expansion. The deployed or folded configurations can be selected based on the application requirement.

Acknowledgments

Y. Chen would like to acknowledge the support from the Nanyang Technological University, Singapore, in the form of a research grant (RG21/05). S.Y. Liu would like to thank URECA program of NTU for providing the financial support in past three years. Authors are grateful to Dr. Z. You in University of Oxford for the valuable comments on the paper.

References

[1] K.H. Hunt, Kinematic Geometry of Mechanisms, Oxford University Press, Oxford, 1978.
[2] P.T. Sarrus, Note sur la transformation des mouvements rectilignes alternatifs, en mouvements circulaires, et reciproquement, Académie des Sciences 36 (1853) 1036–1038.
[3] G.T. Bennett, A new mechanism, Engineering 76 (1903) 777–778.
[4] G.T. Bennett, The skew isogram mechanism, Proceeding of London Mathematics Society, second series, vol. 13, 1914, pp. 151–173.
[5] F.E. Myard, Contribution à la géométrie des systèmes articulés, Societe mathématiques de France 59 (1931) 183–210.
[6] M. Goldberg, New five-bar and six-bar linkages in three dimensions, Trans. ASME 65 (1943) 649–663.
[7] Mavroidis C, Roth B. Analysis and synthesis of overconstrained mechanism, in: Proceedings of the 1994 ASME Design Technical Conference, Minneapolis, MI, September, 1994, pp. 115–133.
[8] P. Dietmaier, A new 6R space mechanism, in: Proceeding 9th World Congress IFToMM, Milano, vol. 1, 1995, pp. 52–56.
[9] K. Wohlhart, Merging two general Goldberg 5R linkages to obtain a new 6R space mechanism, Mechanism and Machine Theory 26 (2) (1991) 659–668.
[10] J.E. Baker, On generating a class of foldable six-bar spatial linkages, Transactions of the ASME, Journal of Mechanical Design 128 (2006) 374–383.
[11] Y. Chen, Z. You, spatial 6R linkages based on the combination of two Goldberg 5R linkages, Mechanism and Machine Theory 42 (11) (2007) 1484–1498.
[12] J.E. Baker, An analysis of Bricard linkages, Mechanism and Machine Theory 15 (1980) 267–286.
[13] J.E. Baker, On 5-revolute linkages with parallel adjacent joint axes, Mechanism and Machine Theory 19 (6) (1984) 467–475.
[14] J.E. Baker, The Bennett, Goldberg and Myard linkages – in perspective, Mechanism and Machine Theory 14 (1979) 239–253.
[15] J.E. Baker, Myard's first five-bar linkage as a degeneracy of a plane-symmetric six-bar loop, Mechanism and Machine Theory 43 (2008) 391–399.
[16] Y. Chen, Z. You, An extended Myard linkage and its derived 6R linkage, Transaction on ASME Journal of Mechanical Design 130 (5) (2008).
[17] S. Briand, Z. You, New deployable mechanisms, Report 2293/07, Department of Engineering Science, University of Oxford, 2007.
[18] B. Grünbaum, G.C. Shephard, Tilings and Patterns, W.H. Freeman and Company, New York, 1986.